Published in final edited form as:
Acta Neuropathol. 2010 January ; 119(1): 123–133. doi:10.1007/s00401-009-0616-y.

Progranulin expression is upregulated after spinal contusion in mice

Swati B. Naphade,
Department of Molecular and Cellular Biochemistry, Center for Molecular Neurobiology, The Ohio State University College of Medicine, Columbus, OH 43210, USA

Kristina A. Kigerl,
Department of Molecular Virology, Immunology and Medical Genetics, Center for Brain and Spinal Cord Repair, The Ohio State University College of Medicine, Columbus, OH 43210, USA

Lyn B. Jakeman,
Department of Cell Biology and Physiology, Center for Brain and Spinal Cord Repair, The Ohio State University College of Medicine, Columbus, OH 43210, USA

Sandra K. Kostyk,
Department of Neurology, Center for Brain and Spinal Cord Repair, The Ohio State University College of Medicine, Columbus, OH 43210, USA

Phillip G. Popovich, and
Department of Molecular Virology, Immunology and Medical Genetics, Center for Brain and Spinal Cord Repair, The Ohio State University College of Medicine, Columbus, OH 43210, USA

Jeff Kuret
Department of Molecular and Cellular Biochemistry, Center for Molecular Neurobiology, The Ohio State University College of Medicine, Columbus, OH 43210, USA

Abstract

Progranulin (proepithelin) is a pleiotropic growth factor associated with inflammation and wound repair in peripheral tissues. It also has been implicated in the response to acute traumatic brain injury as well as to chronic neurodegenerative diseases. To determine whether changes in progranulin expression also accompany acute spinal cord injury, C57BL/6 mice were subjected to mid-thoracic (T9 level) contusion spinal cord injury and analyzed by immunohistochemical and biochemical methods. Whereas spinal cord sections prepared from non-injured laminectomy control animals contained low basal levels of progranulin immunoreactivity in gray matter, sections from injured animals contained intense immunoreactivity throughout the injury epicenter that peaked 7–14 days post injury. Progranulin immunoreactivity colocalized with myeloid cell markers CD11b and CD68, indicating that expression increased primarily in activated microglia and macrophages. Immunoblot analysis confirmed that progranulin protein levels rose after injury. On the basis of quantitative polymerase chain reaction analysis, increased protein levels resulted from a 10-fold rise in progranulin transcripts. These data demonstrate that progranulin is

Correspondence to: Jeff Kuret.
kuret.3@osu.edu, TEL: +1-614-6885899, FAX: +1-614-2925379.

dramatically induced in myeloid cells after experimental spinal cord injury and is positioned appropriately both spatially and temporally to influence recovery after injury.

Keywords

progranulin; spinal cord injury; neurodegeneration; neuroinflammation; trauma

Introduction

Progranulin (GRN) is a secreted ~600 amino acid N-linked glycoprotein growth factor [18]. It is widely expressed in adult mammalian tissues, including brain, with highest levels in cells of epithelial and myeloid origin [12, 13]. In addition to established roles in wound repair in the periphery [19], recent evidence suggests that GRN also has important functions within the central nervous system (CNS). First, purified GRN enhances survival and promotes neurite outgrowth when applied to rat primary cortical and motor neurons in culture, indicating that it has neurotrophic activity [57]. In fact, loss-of-function mutations in *GRN* cause familial frontotemporal lobar degeneration [4, 11, 58], raise the risk of developing Alzheimer's disease [8], and modify the course of amyotrophic lateral sclerosis (ALS) [52]. Second, GRN expression increases in chronic neurodegenerative disorders associated with neuroinflammation, including ALS [37], Creutzfeldt-Jakob disease [3], lysosomal polysaccharide storage disease [41], and Alzheimer's disease [1]. In mouse models of β-amyloid plaque deposition, induction of GRN expression is closely associated with the inflammation that accompanies lesion formation [42]. Finally, GRN expression also increases after acute nervous system injury in rodent models of sciatic axotomy [39] and traumatic brain injury [38]. Together these observations suggest that GRN secretion may influence the survival of diverse neuronal cell populations in response to a wide range of acute and chronic stresses.

The purpose of this study is to extend investigation of GRN expression patterns to a well-characterized model of traumatic spinal cord injury (SCI). As in other CNS regions, acute injury of spinal cord leads to glial activation and scar formation at the site of injury [16]. However, spinal cord supports a more robust inflammatory response than brain tissue owing to greater and deeper infiltration of granulocytes and monocytes after injury along with stronger recruitment and activation of macrophages [15, 49]. Well-characterized SCI models can be especially useful for establishing the kinetics of GRN induction and its relationship to the cascade of inflammatory changes associated with traumatic CNS injury.

Here we show that GRN expression greatly increases in response to experimental SCI in a mouse model, and that microglia and monocyte-derived macrophages are the primary cellular sources of GRN after injury. The results demonstrate that GRN is present at the appropriate time and place to influence neuronal survival and repair after SCI.

Materials and methods

Animals, surgery, and care

Age- and weight-matched female C57BL/6 mice (~20 g) were obtained from Jackson Laboratories (Bar Harbor, ME). All surgical and postoperative care procedures were performed in accordance with The Ohio State University Institutional Animal Care and Use Committee and the National Research Council Guide for the Use and Care of Laboratory Animals. Mice were anesthetized with ketamine (80 mg/kg)/ xylazine (10 mg/kg) prior to receiving a dorsal laminectomy (1.5 mm × 1.7 mm) at the ninth thoracic vertebral level. Laminectomized animals received a moderate spinal contusion injury (0.5 mm displacement) with an electromechanical device as described previously [23, 24, 55]. Postoperatively, animals received prophylactic antibiotics (1 mg/kg Gentacin, s.c.) for 5 days and 2 ml Ringer's solution (s.c.) daily for 5 days to prevent dehydration. Bladders were voided manually twice per day for the duration of the study. Urine pH was monitored weekly throughout the study, and animals were observed daily for signs of infection or abnormal wound healing at the site of surgery. There were no overt signs of infection in any mice.

Tissue preparation

Anesthetized mice were perfused intracardially with 100 ml of 0.1 M phosphate-buffered saline (pH 7.4). For immunohistochemical experiments, animals were further perfused with 100 ml of 4% paraformaldehyde. Spinal cords were postfixed via immersion in 4% paraformaldehyde for 2 h, then rinsed and stored overnight at 4°C in 0.2 M phosphate buffer (pH 7.4). Tissues were then cryoprotected in 20% sucrose for 48 h. Spinal cords were blocked into 1-cm segments centered on the impact site and then embedded in optimal cutting temperature compound (VWR International). Transverse serial sections (14 μm) were cut through each 1-cm block with a cryostat and collected on SuperFrost+ slides (Fisher Scientific, Fair Lawn, NJ) and stored at −20°C until used. Frozen sections were air dried for 2 h, then for an additional 2 h on a slide warmer (37°C). After rinsing (0.2 M phosphate buffer; 1 min), sections were blocked in 4% rabbit serum for 1 h at 4°C.

To prepare homogenates for immunoblot analysis, thoracic spinal cord segments centered on the injury epicenter (4 mm) were dissected from perfused animals and homogenized under nonreducing conditions in 20 volumes/weight of Tissue Protein Extraction Reagent (T-PER™; Pierce, Rockford, IL) and 5 μL Halt™ Protease Inhibitor cocktail (Pierce) using a glass-teflon homogenizer. Aliquots were stored at −70°C until used.

Immunohistochemistry, immunofluorescence, and confocal microscopy

For immunofluorescence experiments, tissue sections were aspirated dry, rinsed, and incubated with the following primary antibodies overnight at 4°C in humidified chambers: sheep anti-mouse GRN (1:1500, R&D Systems Inc.), rat anti-mouse CD68 (1:2000, AbD Serotec), rat anti-mouse CD11b (Mac-1) (1:800, AbD Serotec), and rabbit anti-glial fibrillary acidic protein (DAKO Corp). The following day, sections were washed three times with 0.5 M Tris buffer (pH 7.6) and incubated with Texas red-conjugated donkey anti-sheep IgG (1:400, Santa Cruz Inc), FITC-conjugated goat anti-rat IgG (1:400, Santa Cruz Inc.),

and Cy5-conjugated goat anti-rabbit (1:400 Jackson Immunoresearch, Inc). Labeled sections were washed three times with 0.5 M Tris buffer (pH 7.6), coverslipped with Vectashield (Vector Labs, CA), and viewed in a Leica TCS SL laser-scanning confocal system (40× oil HCX Plan Apo CS 0.75–1.25 NA objective lens) operated at wavelengths optimized for simultaneous detection of FITC (λ_{ex} = 495 nm; λ_{em} = 521 nm), Texas red (λ_{ex} = 589 nm; λ_{em} = 615 nm), and Cy5 (λ_{ex} = 633 nm; λ_{em} = 670 nm). Digital confocal images (Tagged Image Format) were imported into Adobe Photoshop CS4 (Adobe Systems, Inc., San Jose, CA) where background illumination was subtracted from all images, and contrast enhancement was applied to help recreate the tissue as viewed through the microscope.

For immunohistochemistry performed with chromogenic substrate, sections were rinsed once with 0.5 M Tris buffer (pH 7.6), then incubated in 6% H_2O_2/methanol for 15 min to quench endogenous peroxidase activity. H_2O_2-treated sections were again rinsed three times with 0.5 M Tris buffer (pH 7.6) and incubated overnight at 4°C with a polyclonal sheep anti-mouse GRN antibody (1:1500 dilution in 2% rabbit serum) in humidified chambers. Sections were then washed three times with 0.5 M Tris buffer (pH 7.6) and incubated with horseradish peroxidise-labeled rabbit anti-sheep IgG secondary antibody (1:500 dilution in 2% rabbit serum, Kirkegaard and Perry Inc., MD). Bound antibody was visualized by using diaminobenzidine as a substrate. Labeled sections were dehydrated through ascending alcohols, cleared in xylene and coverslipped with Permount (Fisher Scientific). All secondary antibodies were negative for non-specific staining under these conditions, as tested by incubations in the absence of primary antibodies. Photomicrographs were captured on a Zeiss Axiophot upright microscope equipped with a Spot RT-KE slider CCD camera (Diagnostic Instruments, Sterling Heights, MI) and Plan Neofluar 2.5×/0.075 and 20×/0.50 objective lenses.

Proportional area (i.e., the ratio of stained cellular profiles to the total cross-sectional area at the lesion epicenter) was estimated as described previously [14]. Briefly, after the outside border of each image was digitally outlined to exclude the meninges, an arbitrary threshold was applied so that cellular labeling was selected with minimal highlighting of background tissue. The threshold was applied equally to all images, which were analyzed using Image J software (National Institutes of Health, Bethesda, MD).

Recombinant GRN

Full-length mouse GRN cDNA (IMAGE: 40109630; Open Biosystems) was PCR amplified using the primers 5’-CATGCTCGAGCGGCCGCCAGTGTAATGGATATT-3’ (forward) and 5’-CTATGCATCAAGCTTGGTACCGAGC-3’ (reverse). PCR products were digested with *Not*I and *Hin*dIII and ligated into the mammalian expression vector pcDNA3.1(−) (Invitrogen, Carlsbad, CA). The expression plasmid was then transfected into HEK293 cells using the Lipofectamine 2000 (Invitrogen). After 48 h, cells were grown under selection (750 μg/ml G418) until monolayer colonies formed. Colonies were maintained in DMEM containing 10% FBS and 750 μg/ml G418 until cells reached 90% confluency, then transferred to DMEM containing 1.5% FBS, 500 μg/ml G418. Cells and conditioned media were harvested after 72–96 h, with cells being lysed (37°C for 10 min) in 20 mM Tris-HCl, pH 7.4, 140 mM NaCl, 1 mM Na_3NO_4, 10 mM NaF, 0.5% v/v Nonidet P-40, 1 mM EDTA,

1 mM 4-(2-aminoethyl)-benzenesulfonylfluoride, 0.85 μM aprotinin, 40 μM bestatin, 20 μM leupeptin, 15 μM pepstatin A, and 14 μM *trans*-Epoxysuccinyl-L-leucylamido[4-guanidino]butane. Cell lysates were centrifuged at 10,000*g* for 10 min at 4°C and the supernatants were stored at −20°C until used.

GRN Digestion assays

To deglycosylate GRN [46], spinal cord homogenates as well as lysates and conditioned media from HEK293 cells transfected with recombinant mouse GRN were dissolved in 0.5% SDS, heat denatured (100°C for 10 min), then digested with Peptide N-glycosidase F (New England Biolabs Inc., Ipswich, MA) at 37°C for 60 min in 50 mM sodium phosphate buffer (pH 7.5) containing 1% NP-40 nonionic detergent. To proteolytically digest recombinant GRN to granulin peptides, conditioned medium was incubated with human neutrophil elastase (Sigma-Aldrich) in 0.1 M Tris-HCl buffer, pH 8.3, 0.96 M NaCl at 37°C [29, 62].

Immunoblot analysis

Aliquots of cell lysates, conditioned media, and tissue homogenates were denatured under reducing conditions (1.75% SDS, 15 mM 2-mercaptoethanol; 3 min at 100°C), then subjected to SDS-PAGE and immunoblot analysis as described previously [32]. To detect GRN, PVDF membranes were incubated with sheep anti-GRN primary antibody (1:1000, overnight at 4°C) then with rabbit anti-sheep IgG conjugated to horseradish peroxidase (1:1000; Kirkegaard and Perry Inc., MD) for 2 h. Immunolabeling was detected with the ECL Western Blotting Analysis System (GE Healthcare, Buckinghamshire, UK). Chemiluminescence was recorded on an Omega 12iC Molecular Imaging System and quantified using UltraQuant software (UltraLum, Claremont, CA). GRN immunoreactivity was normalized to total protein as determined by Bradford assay [7] (Bio-Rad Laboratories, Inc., Hercules, CA). β3-Tubulin immunoreactivity, detected with monoclonal antibody TuJ1 [31] and a goat anti-mouse IgG secondary antibody conjugated to horseradish peroxidase (1:5000; Kirkegaard and Perry), served as a loading control.

RNA analysis

RNA was prepared from thoracic spinal cord segments (centered on the injury epicenter) as described previously [26] and characterized in an Agilent 2100 bioanalyzer. Samples had RNA integrity numbers (a measure of RNA quality; [50]) ranging from 7.7 – 9.9 (average of 8.8 ± 0.7) and rRNA ratios (i.e., 28S/18S rRNA) ranging from 1.1 – 1.8 (average of 1.4 ± 0.2). For microarray analysis, each condition included four unpooled replicates, each measured on a separate array. Separate microarrays also examined individual RNA samples from laminectomy control animals. The hybridization target was prepared using the Genisphere 3DNA dendrimer system (Genisphere, Inc., Hatfield, PA, USA). Total cellular RNA (2 μg) was reverse transcribed from a ‘capture sequence’-containing oligo d(T)18 primer using Superscript II (Invitrogen) and then alkaline hydrolyzed to destroy RNA. Automated hybridizations were performed using a Ventana Discovery System (Ventana Medical Systems, Tuscon, AZ, USA) [9].

To quantify GRN mRNA expression, cDNA was prepared from tissue-derived RNA and then subjected to quantitative real-time PCR as described previously [26]. PCR reactions contained 10 ng of cDNA, SYBR Green master mix (QuantiTect SYBR Green RT-PCR kit, Qiagen, Valencia, CA, USA), and 500 nmol/L each of the primers 5'-GTTCACACACATGCGTTTCA-3' (forward) and 5'-CCCTGTTGGTCTTTTGTGCAG-3' (reverse) in 20 μL (final volume). Levels of SYBR-Green labeled PCR products were quantified on an Applied Biosystems 7300 system [47]. Melting point analyses were performed for each reaction to confirm single amplified products. Real time data were analysed by the comparative C_T method [48], where C_T is defined as the PCR cycle at which the fluorescent signal of the reporter dye crosses an arbitrarily placed threshold. Fold change is reported as $2^{-\Delta\Delta C_T}$ [48], with endogenous 18S rRNA serving as the internal reference [26].

Statistical analysis

All measured parameters are reported as means ± S.D. of 3 – 6 replicates. Differences among laminectomy control and injured groups were analyzed by one-way ANOVA and Dunnett's post hoc multiple comparison test using Prism 4.03 (GraphPad Software, Inc., La Jolla, CA). The null hypothesis was rejected at $p < 0.05$.

Results

Antibody selectivity

To characterize the specificity of a polyclonal anti-mouse GRN antibody, cell homogenates and conditioned media from HEK293 cells transiently transfected with an expression vector (pcDNA3.1) containing no insert or full-length mouse GRN cDNA (accession number NP_032201) were subjected to immunoblot analysis. HEK293 cells were chosen for characterization because heterologous expression of GRN in mammalian cells reportedly preserves its mature glycosylation state [62]. Neither whole-cell lysates nor conditioned media from cells transfected with empty vector contained GRN immunoreactivity (Fig. 1a). However, cells transfected with pcDNA3.1-GRN yielded strong anti-GRN immunoreactivity that migrated as species with molecular masses of ~78 kDa and ~88 kDa. The former species predominated in cell lysates, whereas the latter was the major variant secreted into conditioned media (Fig 1a). When digested with Peptide N-glycosidase F (an enzyme capable of deglycosylating the N-linked glycans of GRN, [46, 61]), immunoreactivity in both cell lystates and conditioned media shifted toward the molecular mass predicted for non-glycosylated mouse GRN (~65 kDa; Fig. 1a). These data suggested that the ~78 kDa and ~88 kDa species corresponded to immature and mature N-glycosylated GRN variants, respectively [51]. They also indicated that the polyclonal anti-GRN antibody was selective for GRN relative to other glycoproteins present in HEK293 cells or in fetal bovine serum containing media, and that it bound both N-glycosylated and nonglycosylated GRN.

GRN is composed of seven and one half imperfect tandem repeats of a cysteine-rich granulin motif separated by short intervening spacer sequences [6, 22, 43]. Cleavage of the linker sequences in mature GRN by neutrophil elastase releases granulin peptides, which

also are bioactive [25, 62]. To determine whether the polyclonal anti-GRN antibody also reacted with granulin peptides, recombinant full-length GRN from conditioned media of pcDNA3.1-GRN transfected cells was digested with increasing concentrations of neutrophil elastase and subjected to immunoblot analysis. Gradient acrylamide gels (10 – 20% acrylamide) were used for this experiment so as to resolve individual granulin peptides down to 6.5 kDa [54]. After incubation in the absence of neutrophil elastase, GRN continued to migrate at ~88 kDa (Fig. 1b). However, incubation in the presence of elastase greatly attenuated immunoreactivity appearing at ~88 kDa without generating significant immunoreactivity in the 6 – 25 kDa region inhabited by granulin peptides (Fig. 1b). Together these data indicate that the polyclonal anti-GRN antibody used herein is highly selective for intact GRN relative to granulin peptides.

GRN is upregulated in response to spinal cord injury

To determine whether GRN expression changed in response to SCI, C57BL/6 mice were subjected to moderate mid-thoracic contusion injury at T9 level, and spinal cord sections prepared at the level of the injury epicenter at 1, 3, 7, 14, 28, and 56 dpi were labeled with the anti-GRN antibody. This model was chosen because contusion is the most common form of spinal cord injury in humans [60]. Moreover, the sequence of anatomical, immune, and behavioral responses has been well characterized in C57BL/6 mice, where moderate injury spares marginal white matter while permitting partial recovery of function after injury [35]. In uninjured laminectomy control animals, GRN immunoreactivity was very low (Fig. 2a, b). In contrast, sections from injured animals revealed punctate immunoreactivity, with prominent clusters of GRN-expressing cells occupying both gray and white matter regions by 3 dpi (Fig. 2c, d). GRN immunoreactivity was maximal between 7–14 dpi (only 14 dpi shown in Fig. 2e, f) where it filled the entire lesion core and extended into the peripheral white matter regions. The staining persisted at later time points, but was mostly confied to the lesion core after glial scar formation (Fig. 2g), with occasional profiles scattered throughout the peripheral rim of spared white matter, especially in the more ventral regions (shown only for 56 dpi in Fig. 2g, h).

These data indicate that GRN levels and distribution change after contusion SCI. To further characterize the changes, immunostaining was quantified from replicate sections collected at each time point post injury. Because counting of individual cells is problematic in the contused spinal cord owing to the clustering of microglia, macrophages and astrocytes [27, 45], GRN labeling was quantified as proportional area, defined as the ratio of the area occupied by GRN immunopositive cellular profiles to the total cross-sectional area of the tissue section [27, 45]. A plot of proportional area versus time revealed a biphasic expression pattern, with upregulation of immunoreactivity peaking at 7–14 dpi followed by decreasing but still elevated levels up to 56 dpi (Fig. 2i). These data indicate that GRN expression increases in response to contusion SCI, and that the time course of increase matches the activation of resident microglia and macrophages derived from infiltrating monocytes [27, 44].

GRN induction time course

To determine whether changes in GRN immunohistochemistry were reflected at the protein level, SCI homogenates prepared 1, 3, 7, 14 and 28 dpi were subjected to immunoblot analysis using the same anti-GRN primary antibody. Homogenates contained immunoreactivity that migrated with molecular masses of ~88 kDa and ~78 kDa, consistent with mature and immature GRN variants identified in HEK293 cells (Fig. 3a). Although the basal level of GRN immunoreactivity in laminectomy control homogenate was barely detectable, large increases in GRN expression followed contusion injury. The time course paralleled the biphasic immunostaining pattern observed in tissue sections, with a robust 9.9 ± 1.6 (n = 3) fold increase in GRN levels detected by 7 dpi followed by decreased but still elevated levels after 28 dpi (Fig. 3b). GRN immunoreactivity at peak induction (7 dpi) migrated primarily at ~78 kDa and was sensitive to Peptide N-glycosidase F, consistent with the behavior of immature GRN associated with actively expressing cells (Fig. 3c). These data confirmed that the immunostaining seen in tissue sections by immunohistochemistry resulted from increased levels of GRN polypeptide, and that the peak of induction occurred ~7 dpi.

Induced GRN colocalizes with macrophage/microglial markers

The time course of GRN induction was consistent with activated microglia and macrophages derived from infiltrating monocytes being major sources of increased GRN expression. To test this hypothesis, double-label immunofluorescence was performed with anti-GRN polyclonal antibody (detected with Texas red-linked secondary antibody) and antibodies raised against CD11b (detected with FITC-linked secondary antibody). CD11b (macrophage-1 antigen; Mac-1) is expressed on the surface of many leukocytes (including monocytes, granulocytes, macrophages and natural killer cells) where it regulates leukocyte adhesion and migration as well as phagocytosis and cell-mediated cytotoxicity [53]. Double-label immuno-fluorescence revealed punctate GRN staining within cell membranes labeled by anti-CD11b (Fig. 4). By 14 dpi, the injury epicenter contained numerous $CD11b^+/GRN^+$ profiles distributed throughout the lesion center and much of the surrounding white matter (Fig. 4a–c). Colocalization of $CD11b^+/GRN^+$ persisted through 56 dpi (Fig. 4d–f). The distinct border region that separated the lesion core from white matter at this time was devoid of GRN labeling, suggesting that activated astrocytes associated with the glial scar did not express GRN. Double-label immunofluorescence with anti-GRN polyclonal antibody and antibody against glial fibrillary acidic protein (GFAP), a marker for hypertrophic astrocytes, confirmed that these astrocytes did not express GRN (data not shown).

The GRN labeling within $CD11b^+$ cell profiles suggests that myeloid cells were the primary cellular sources of GRN immunoreactivity after injury and that GRN localized within activated microglia/macrophages. To test this hypothesis, double-label immunofluorescence was performed with anti-GRN polyclonal antibody (detected with Texas red-linked secondary antibody) and antibodies raised against CD68 (detected with FITC-linked secondary antibody). CD68 is a pan-macrophage antigen expressed throughout monocyte differentiation; however, it is strongly upregulated in activated macrophages relative to undifferentiated monocytes [21]. It is a member of the lysosomal/endosomal-associated

membrane glycoprotein family, and shuttles between cytoplasmic granules and the cell surface [20, 30]. The punctate GRN staining pattern largely colocalized with intracellular CD68 staining (shown at 28 dpi in Fig. 5). Together, double-label immunofluorescence results with GRN/CD11b and GRN/CD68 indicate that GRN is expressed by cells of myeloid lineage and specifically upregulated in activated macrophages and microglia in response to contusion SCI.

Mechanism

To determine the mechanism through which contusion injury leads to GRN upregulation, levels of GRN RNA were assayed in the spinal cords of injured animals as a function of time post-injury by microarray and quantitative PCR analysis. Both methods revealed a biphasic increase in GRN transcripts that peaked at 7 dpi and that paralleled GRN immunoreactivity in tissue homogenates (Fig. 6). At peak expression, array analysis estimated a log 2 ratio of 3.57 ± 0.12, which corresponds to a 11.9 ± 1.0 fold increase compared to laminectomy control (Fig. 6a). Relative to 18S RNA, which served as an internal standard in quantitative PCR experiments, GRN transcripts maximally increased 9.6 ± 2.0 fold (quadruplicate determination) 7 dpi when compared to laminectomy control (Fig. 6b). However, expression levels remained significantly elevated for at least 28 dpi. Together these data revealed that GRN mRNA expression increased by an order of magnitude following contusion SCI, that this induction resulted in large increases in GRN protein levels, and that activated microglia and macrophages were the principal source of GRN.

Discussion

Neural injury following spinal contusion results from primary damage (*i.e*., acute mechanical shearing and stretching of axons and blood vessels) as well as from a cascade of secondary processes that leads to disruption of the blood-brain barrier and extracellular matrix, progressive lesion expansion, glial scar formation, and delayed demyelination [16]. Although primary injury is rapid and irreversible, secondary injury develops over time and is modulated by cellular and humoral effectors of inflammation. Here we found that GRN expression varies with the inflammatory response to contusion SCI. In conjunction with its established role in wound healing in peripheral tissues [19, 62], the data implicate GRN as a candidate factor for modulating secondary injury as well as subsequent repair or regeneration of injured spinal cord.

First, induction of GRN expression places elevated concentrations of GRN at the injury epicenter. A robust induction of GRN expression has been reported in other injury models as well. For example, shortly after transcutaneous puncture injury, GRN mRNA levels increase and remain above baseline for at least 10 dpi [19]. Although the signal for induction after SCI has not been established, the promoter for both human [5] and murine [2] GRN contains potential inflammation-related regulatory elements involved in cytokine and growth-factor regulated gene expression [5]. For example, interleukin1β (IL-1β) and tumor necrosis factor-α (TNFα), two pro-inflammatory cytokines of the innate immune system, activate *GRN* expression in murine embryo fibroblasts through nuclear factor κB [33].

Second, GRN levels are elevated during the time that secondary injury and tissue repair occur. The timing of GRN induction most closely parallels the reported time course of microglial activation and monocyte-derived macrophage infiltration, with peak induction 7 dpi correlating with the peak of the microglial/macrophage response [15]. In agreement with this timing, GRN colocalized with CD68, a marker enriched in activated macrophages and microglia. These results are consistent with activated microglia and macrophages being the predominant cellular sources of GRN expression in injured peripheral tissues [28, 59] and in the brains of individuals suffering from neurodegenerative disorders [3, 40], including frontotemporal lobar degeneration [4, 10, 36]. Although GRN is a modulator of macrophage proliferation [17], it also supports an anti-inflammatory phenotype of various cell types. For example, GRN has been reported to antagonize TNFα-mediated IL8 secretion from a human monocytic leukemia cell line [28]. The anti-inflammatory effects of GRN suggest one mechanism through which GRN expression may influence the course of secondary injury.

Finally, GRN possesses growth factor activity capable of directly influencing repair of tissues after injury. For example, GRN administered to a fresh transcutaneous wound reportedly stimulates fibroblast proliferation and new blood vessel formation, both of which are essential for repair [19]. GRN stimulates tubule formation to the same extent as fibroblast growth factor-2, suggesting that the neovascularization accompanying GRN administration is at least partly due to direct angiogenic action [18, 19]. Other studies using primary cortical and spinal motor neuron cultures demonstrated that GRN is a neurotrophic factor that enhances neuronal survival and axonal outgrowth [57]. The severe neurodegenerative phenotype observed in several FTLD cases associated with GRN null mutations/haploinsufficiency has been attributed to the loss of this neurotrophic support [1]. The neurotrophic and angiogenic activity associated with GRN may aid repair after SCI.

The spectrum of GRN-mediated biological effects depends not only on its levels of expression and timing of secretion, but also on its degree of postranslational modification. Indeed, proteolytic cleavage of GRN into its constituent granulin peptides yields products with separate and sometimes mutually antagonizing activities [25, 28, 62]. Secreted proteases including elastase-2 and proteinase-3 catalyze this reaction [25]. Conversely, secretory leukocyte protease inhibitor (SLPI) prevents GRN processing through inhibition of elastase enzymatic activity and by binding GRN at the inter-GRN linker regions and thus sequestering it from elastase [62]. Interplay among these factors modulates the balance between GRN and granulin peptides. For example, SLPI null mice have decreased GRN levels (owing to elevated elastase secretion) and impaired wound healing. Administration of recombinant GRN to these animals restored wound healing [62]. Our study did not capture the processing of GRN to granulin peptides because the anti-GRN antibody used for immunostaining was selective for fulllength protein. However, the reported ability of a neutrophil elastase inhibitor to reduce neurologic damage after experimental SCI in rats [56] suggests that this aspect of GRN biology should be addressed in future studies.

In summary, these data add to a growing literature implicating GRN in the inflammatory events that follow injury in the CNS. The data presented herein suggest that GRN is a candidate modulator of secondary injury and repair after contusion SCI, and a new avenue for intervention to improve recovery after SCI.

Acknowledgments

We thank Dr. Mariano Viapiano (Department of Neurosurgery) for guidance with imaging methods. This work was supported by The Ohio State University Neuroscience Signature Program (S.K.K., L.B.J., J.K.), National Institute for Neurological Disorders and Stroke (P.G.P.), Neuroscience Core Center (NS045758), and The Ohio State Center for Brain and Spinal Cord Repair.

References

1. Ahmed Z, Mackenzie IR, Hutton ML, Dickson DW. Progranulin in frontotemporal lobar degeneration and neuroinflammation. J Neuroinflammation. 2007; 4:7. [PubMed: 17291356]
2. Baba T, Hoff HB 3rd, Nemoto H, et al. Acrogranin, an acrosomal cysteine-rich glycoprotein, is the precursor of the growth-modulating peptides, granulins, and epithelins, and is expressed in somatic as well as male germ cells. Mol Reprod Dev. 1993; 34:233–243. [PubMed: 8471244]
3. Baker CA, Manuelidis L. Unique inflammatory RNA profiles of microglia in Creutzfeldt-Jakob disease. Proc Natl Acad Sci U S A. 2003; 100:675–679. [PubMed: 12525699]
4. Baker M, Mackenzie IR, Pickering-Brown SM, et al. Mutations in progranulin cause tau-negative frontotemporal dementia linked to chromosome 17. Nature. 2006; 442:916–919. [PubMed: 16862116]
5. Bhandari V, Daniel R, Lim PS, Bateman A. Structural and functional analysis of a promoter of the human granulin/epithelin gene. Biochem J. 1996; 319:441–447. [PubMed: 8912679]
6. Bhandari V, Palfree RG, Bateman A. Isolation and sequence of the granulin precursor cDNA from human bone marrow reveals tandem cysteine-rich granulin domains. Proc Natl Acad Sci U S A. 1992; 89:1715–1719. [PubMed: 1542665]
7. Bradford MM. A rapid and sensitive method for the quantitation of microgram quantities of protein utilizing the principle of protein-dye binding. Anal Biochem. 1976; 72:248–254. [PubMed: 942051]
8. Brouwers N, Sleegers K, Engelborghs S, et al. Genetic variability in progranulin contributes to risk for clinically diagnosed Alzheimer disease. Neurology. 2008; 71:656–664. [PubMed: 18565828]
9. Carmel JB, Kakinohana O, Mestril R, Young W, Marsala M, Hart RP. Mediators of ischemic preconditioning identified by microarray analysis of rat spinal cord. Exp Neurol. 2004; 185:81–96. [PubMed: 14697320]
10. Chen-Plotkin AS, Xiao J, Geser F, et al. Brain progranulin expression in GRN-associated frontotemporal lobar degeneration. Acta Neuropathol. 2009 in press.
11. Cruts M, Gijselinck I, van der Zee J, et al. Null mutations in progranulin cause ubiquitin-positive frontotemporal dementia linked to chromosome 17q21. Nature. 2006; 442:920–924. [PubMed: 16862115]
12. Daniel R, Daniels E, He Z, Bateman A. Progranulin (acrogranin/PC cell-derived growth factor/granulin-epithelin precursor) is expressed in the placenta, epidermis, microvasculature, and brain during murine development. Dev Dyn. 2003; 227:593–599. [PubMed: 12889069]
13. Daniel R, He Z, Carmichael KP, Halper J, Bateman A. Cellular localization of gene expression for progranulin. J Histochem Cytochem. 2000; 48:999–1009. [PubMed: 10858277]
14. Donnelly DJ, Gensel JC, Ankeny DP, van Rooijen N, Popovich PG. An efficient and reproducible method for quantifying macrophages in different experimental models of central nervous system pathology. J Neurosci Meth. 2009; 181:36–44.
15. Donnelly DJ, Popovich PG. Inflammation and its role in neuroprotection, axonal regeneration and functional recovery after spinal cord injury. Exp Neurol. 2008; 209:378–388. [PubMed: 17662717]
16. Fitch MT, Silver J. CNS injury, glial scars, and inflammation: Inhibitory extracellular matrices and regeneration failure. Exp Neurol. 2008; 209:294–301. [PubMed: 17617407]
17. Hanington PC, Barreda DR, Belosevic M. A novel hematopoietic granulin induces proliferation of goldfish (Carassius auratus L.) macrophages. J Biol Chem. 2006; 281:9963–9970. [PubMed: 16473876]

18. He Z, Bateman A. Progranulin (granulin-epithelin precursor, PC-cell-derived growth factor, acrogranin) mediates tissue repair and tumorigenesis. J Mol Med. 2003; 81:600–612. [PubMed: 12928786]
19. He Z, Ong CH, Halper J, Bateman A. Progranulin is a mediator of the wound response. Nat Med. 2003; 9:225–229. [PubMed: 12524533]
20. Holness CL, da Silva RP, Fawcett J, Gordon S, Simmons DL. Macrosialin, a mouse macrophage-restricted glycoprotein, is a member of the lamp/lgp family. J Biol Chem. 1993; 268:9661–9666. [PubMed: 8486654]
21. Holness CL, Simmons DL. Molecular cloning of CD68, a human macrophage marker related to lysosomal glycoproteins. Blood. 1993; 81:1607–1613. [PubMed: 7680921]
22. Hrabal R, Chen Z, James S, Bennett HP, Ni F. The hairpin stack fold, a novel protein architecture for a new family of protein growth factors. Nat Struct Biol. 1996; 3:747–752. [PubMed: 8784346]
23. Jakeman LB, Guan Z, Wei P, et al. Traumatic spinal cord injury produced by controlled contusion in mouse. J Neurotrauma. 2000; 17:299–319. [PubMed: 10776914]
24. Jones TB, Basso DM, Sodhi A, et al. Pathological CNS autoimmune disease triggered by traumatic spinal cord injury: implications for autoimmune vaccine therapy. J Neurosci. 2002; 22:2690–2700. [PubMed: 11923434]
25. Kessenbrock K, Frohlich L, Sixt M, et al. Proteinase 3 and neutrophil elastase enhance inflammation in mice by inactivating antiinflammatory progranulin. J Clin Invest. 2008; 118:2438–2447. [PubMed: 18568075]
26. Kigerl KA, Lai W, Rivest S, Hart RP, Satoskar AR, Popovich PG. Toll-like receptor (TLR)-2 and TLR-4 regulate inflammation, gliosis, and myelin sparing after spinal cord injury. J Neurochem. 2007; 102:37–50. [PubMed: 17403033]
27. Kigerl KA, McGaughy VM, Popovich PG. Comparative analysis of lesion development and intraspinal inflammation in four strains of mice following spinal contusion injury. J Comp Neurol. 2006; 494:578–594. [PubMed: 16374800]
28. Kojima Y, Ono K, Inoue K, et al. Progranulin expression in advanced human atherosclerotic plaque. Atherosclerosis. 2009; 206:102–108. [PubMed: 19321167]
29. Kramps JA, van Twisk C, van der Linden AC. L-Pyroglutamyl-L-prolyl-L-valine-pnitroanilide, a highly specific substrate for granulocyte elastase. Scand J Clin Lab Invest. 1983; 43:427–432. [PubMed: 6557666]
30. Kurushima H, Ramprasad M, Kondratenko N, Foster DM, Quehenberger O, Steinberg D. Surface expression and rapid internalization of macrosialin (mouse CD68) on elicited mouse peritoneal macrophages. J Leukoc Biol. 2000; 67:104–108. [PubMed: 10648004]
31. Lee MK, Tuttle JB, Rebhun LI, Cleveland DW, Frankfurter A. The expression and posttranslational modification of a neuron-specific beta-tubulin isotype during chick embryogenesis. Cell Motil Cytoskeleton. 1990; 17:118–132. [PubMed: 2257630]
32. Li G, Yin H, Kuret J. Casein kinase 1 delta phosphorylates tau and disrupts its binding to microtubules. J Biol Chem. 2004; 279:15938–15945. [PubMed: 14761950]
33. Li X, Massa PE, Hanidu A, et al. IKKalpha, IKKbeta, and NEMO/IKKgamma are each required for the NF-kappa B-mediated inflammatory response program. J Biol Chem. 2002; 277:45129–45140. [PubMed: 12221085]
34. Liu NK, Xu XM. β-tubulin is a more suitable internal control than β-actin in western blot analysis of spinal cord tissues after traumatic injury. J Neurotrauma. 2006; 23:1794–1801. [PubMed: 17184189]
35. Ma M, Basso DM, Walters P, Stokes BT, Jakeman LB. Behavioral and histological outcomes following graded spinal cord contusion injury in the C57Bl/6 mouse. Exp Neurol. 2001; 169:239–254. [PubMed: 11358439]
36. Mackenzie IR, Baker M, Pickering-Brown S, et al. The neuropathology of frontotemporal lobar degeneration caused by mutations in the progranulin gene. Brain. 2006; 129:3081–3090. [PubMed: 17071926]
37. Malaspina A, Kaushik N, de Belleroche J. Differential expression of 14 genes in amyotrophic lateral sclerosis spinal cord detected using gridded cDNA arrays. J Neurochem. 2001; 77:132–145. [PubMed: 11279269]

38. Matzilevich DA, Rall JM, Moore AN, Grill RJ, Dash PK. High-density microarray analysis of hippocampal gene expression following experimental brain injury. J Neurosci Res. 2002; 67:646–663. [PubMed: 11891777]
39. Moisse K, Volkening K, Leystra-Lantz C, Welch I, Hill T, Strong MJ. Divergent patterns of cytosolic TDP-43 and neuronal progranulin expression following axotomy: implications for TDP-43 in the physiological response to neuronal injury. Brain Res. 2009; 1249:202–211. [PubMed: 19046946]
40. Mukherjee O, Pastor P, Cairns NJ, et al. HDDD2 is a familial frontotemporal lobar degeneration with ubiquitin-positive, tau-negative inclusions caused by a missense mutation in the signal peptide of progranulin. Ann Neurol. 2006; 60:314–322. [PubMed: 16983685]
41. Ohmi K, Greenberg DS, Rajavel KS, Ryazantsev S, Li HH, Neufeld EF. Activated microglia in cortex of mouse models of mucopolysaccharidoses I and IIIB. Proc Natl Acad Sci U S A. 2003; 100:1902–1907. [PubMed: 12576554]
42. Pereson S, Wils H, Kleinberger G, et al. Progranulin expression correlates with dense-core amyloid plaque burden in Alzheimer disease mouse models. J Pathol. 2009; 219:173–181. [PubMed: 19557827]
43. Plowman GD, Green JM, Neubauer MG, et al. The epithelin precursor encodes two proteins with opposing activities on epithelial cell growth. J Biol Chem. 1992; 267:13073–13078. [PubMed: 1618805]
44. Popovich PG, Hickey WF. Bone marrow chimeric rats reveal the unique distribution of resident and recruited macrophages in the contused rat spinal cord. J Neuropathol Exp Neurol. 2001; 60:676–685. [PubMed: 11444796]
45. Popovich PG, Wei P, Stokes BT. Cellular inflammatory response after spinal cord injury in Sprague-Dawley and Lewis rats. J Comp Neurol. 1997; 377:443–464. [PubMed: 8989657]
46. Qin J, Diaz-Cueto L, Schwarze JE, et al. Effects of progranulin on blastocyst hatching and subsequent adhesion and outgrowth in the mouse. Biol Reprod. 2005; 73:434–442. [PubMed: 15901638]
47. Ririe KM, Rasmussen RP, Wittwer CT. Product differentiation by analysis of DNA melting curves during the polymerase chain reaction. Anal Biochem. 1997; 245:154–160. [PubMed: 9056205]
48. Schmittgen TD, Livak KJ. Analyzing real-time PCR data by the comparative C(T) method. Nat Protoc. 2008; 3:1101–1108. [PubMed: 18546601]
49. Schnell L, Fearn S, Klassen H, Schwab ME, Perry VH. Acute inflammatory responses to mechanical lesions in the CNS: differences between brain and spinal cord. Eur J Neurosci. 1999; 11:3648–3658. [PubMed: 10564372]
50. Schroeder A, Mueller O, Stocker S, et al. The RIN: an RNA integrity number for assigning integrity values to RNA measurements. BMC Mol Biol. 2006; 7:3. [PubMed: 16448564]
51. Shankaran SS, Capell A, Hruscha AT, et al. Missense mutations in the progranulin gene linked to frontotemporal lobar degeneration with ubiquitin-immunoreactive inclusions reduce progranulin production and secretion. J Biol Chem. 2008; 283:1744–1753. [PubMed: 17984093]
52. Sleegers K, Brouwers N, Maurer-Stroh S, et al. Progranulin genetic variability contributes to amyotrophic lateral sclerosis. Neurology. 2008; 71:253–259. [PubMed: 18184915]
53. Solovjov DA, Pluskota E, Plow EF. Distinct roles for the alpha and beta subunits in the functions of integrin alphaMbeta2. J Biol Chem. 2005; 280:1336–1345. [PubMed: 15485828]
54. Sparro G, Galdenzi G, Eleuteri AM, Angeletti M, Schroeder W, Fioretti E. Isolation and N-terminal sequence of multiple forms of granulins in human urine. Protein Expr Purif. 1997; 10:169–174. [PubMed: 9226711]
55. Sroga JM, Jones TB, Kigerl KA, McGaughy VM, Popovich PG. Rats and mice exhibit distinct inflammatory reactions after spinal cord injury. J Comp Neurol. 2003; 462:223–240. [PubMed: 12794745]
56. Tonai T, Shiba K, Taketani Y, et al. A neutrophil elastase inhibitor (ONO-5046) reduces neurologic damage after spinal cord injury in rats. J Neurochem. 2001; 78:1064–1072. [PubMed: 11553680]

57. Van Damme P, Van Hoecke A, Lambrechts D, et al. Progranulin functions as a neurotrophic factor to regulate neurite outgrowth and enhance neuronal survival. J Cell Biol. 2008; 181:37–41. [PubMed: 18378771]

58. van der Zee J, Le Ber I, Maurer-Stroh S, et al. Mutations other than null mutations producing a pathogenic loss of progranulin in frontotemporal dementia. Hum Mutat. 2007; 28:416. [PubMed: 17345602]

59. Youn BS, Bang SI, Kloting N, et al. Serum progranulin concentrations may be associated with macrophage infiltration into omental adipose tissue. Diabetes. 2009; 58:627–636. [PubMed: 19056610]

60. Young W. Spinal cord contusion models. Prog Brain Res. 2002; 137:231–255. [PubMed: 12440371]

61. Zhou J, Gao G, Crabb JW, Serrero G. Purification of an autocrine growth factor homologous with mouse epithelin precursor from a highly tumorigenic cell line. J Biol Chem. 1993; 268:10863–10869. [PubMed: 8496151]

62. Zhu J, Nathan C, Jin W, et al. Conversion of proepithelin to epithelins: roles of SLPI and elastase in host defense and wound repair. Cell. 2002; 111:867–878. [PubMed: 12526812]

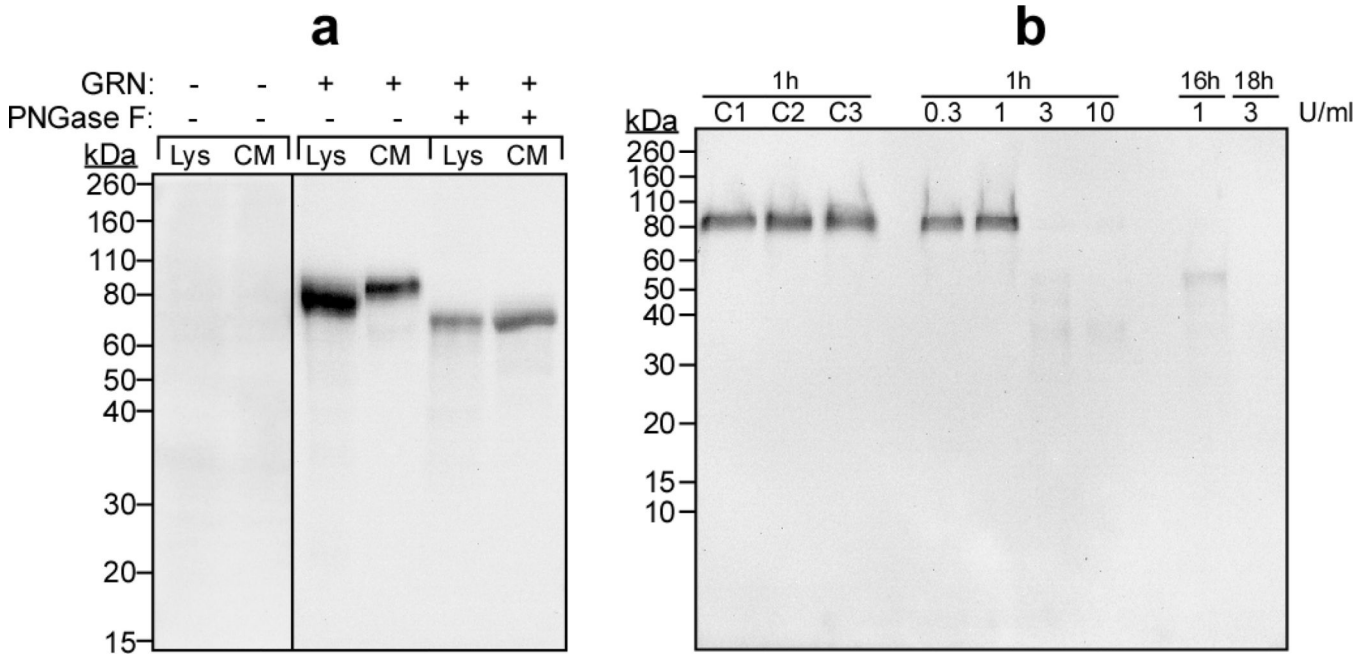

Fig. 1. Anti-GRN antibody detects full-length GRN

(**a**) Whole-cell lysates (Lys) and conditioned media (CM) were prepared from HEK293 cells transfected with expression vector pcDNA3.1 alone (GRN −) or pcDNA3.1-GRN (GRN +). Samples were then incubated in the presence or absence of Peptide N-glycosidase F (PNGase F) followed by immunoblot analysis (10% acrylamide gel) with polyclonal anti-mouse GRN antibody (1:1000). The resultant staining pattern was calibrated with prestained molecular mass standards (shown in units of kDa on left). Antibody reactivity was detected only in lysates and conditioned media prepared from cells transfected with pcDNA3.1-GRN, and was retained after deglycosylation with Peptide N-glycosidase F. (**b**) Recombinant mouse GRN (5.0 μl conditioned media) was incubated (37°C) for up to 18 h in the presence of human neutrophil elastase (0.3, 1, 3, or 10 U/ml), then subjected to immunoblot analysis (10 – 20% gradient acrylamide gel) with anti-GRN antibody. Control reactions included C1 (no elastase, incubation at 0°C); C2 (elastase was added to the reaction mixture and sample was boiled immediately); and C3 (no elastase, incubation at 37°C for 60 min). Elastase-mediated cleavage of GRN greatly attenuated antibody reactivity relative to control reactions.

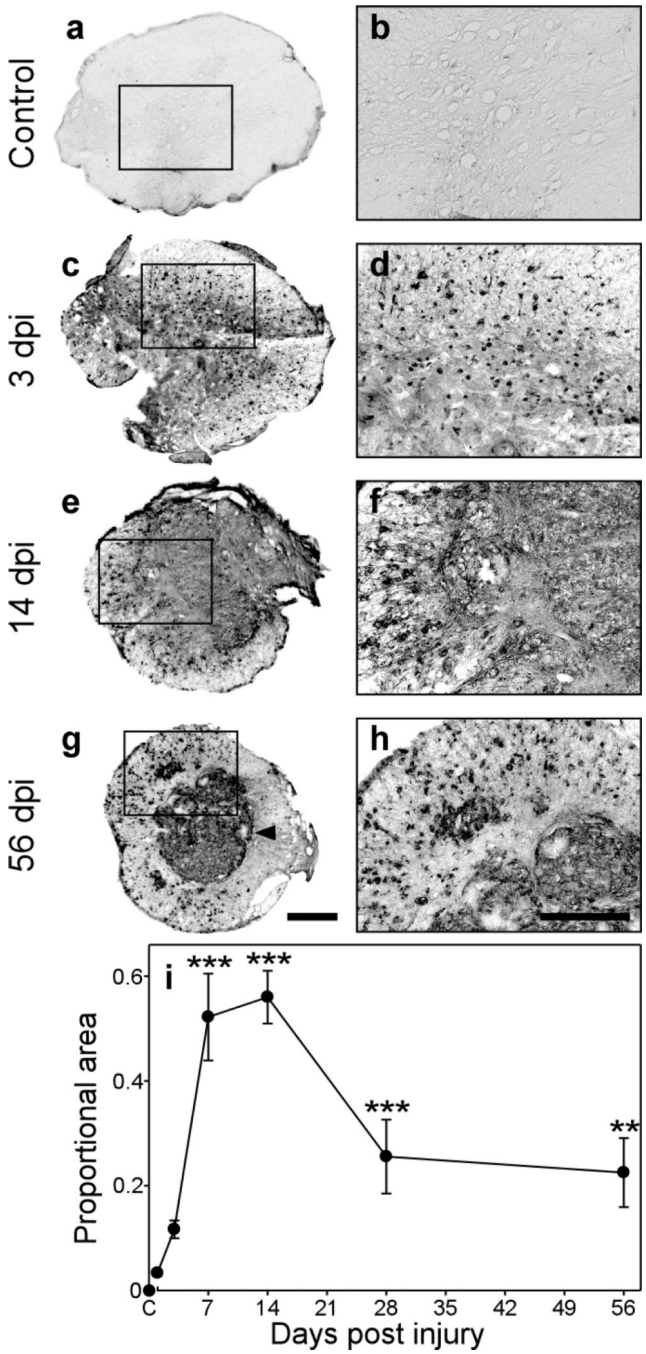

Fig. 2. GRN immunoreactivity increases after contusion SCI

Transverse sections prepared from a laminectomy control (**a, b**) and injured (**c–h**) C57BL/6 mice were subjected to immunohistochemistry using anti-GRN antibody and chromogenic substrate diaminobenzidine. Labeled sections are shown at the level of the injury epicenter at low magnification in panels **a, c, e, g** (scale bar = 250 μm), with the boxed regions shown at 4-fold higher magnification in panels **b, d, f, h** (scale bar = 125 μm). In the absence of contusion injury (**a, b**), basal GRN immunoreactivity was diffuse and appeared primarily in gray matter. After contusion injury (**c – h**), GRN immunoreactivity greatly increased with

time at the lesion epicenter, and by 14 dpi occupied most of the cross-sectional area. At later time points (**g, h**), after formation of the glial scar (*arrowhead* in **g**), GRN labeling was mostly confined to the lesion core with modest labeling in the spared peripheral white matter. (**i**) The proportional area (PA) of each tissue section occupied by GRN immunoreactivity was quantified ± SD and plotted as a function of time (three sections/animal; three animals/time point). Proportional area increased significantly after injury and was maximal between 7 and 14 dpi (**, $p < 0.01$; ***, $p < 0.001$ compared to the laminectomy control group; ANOVA with Dunnett's post hoc test).

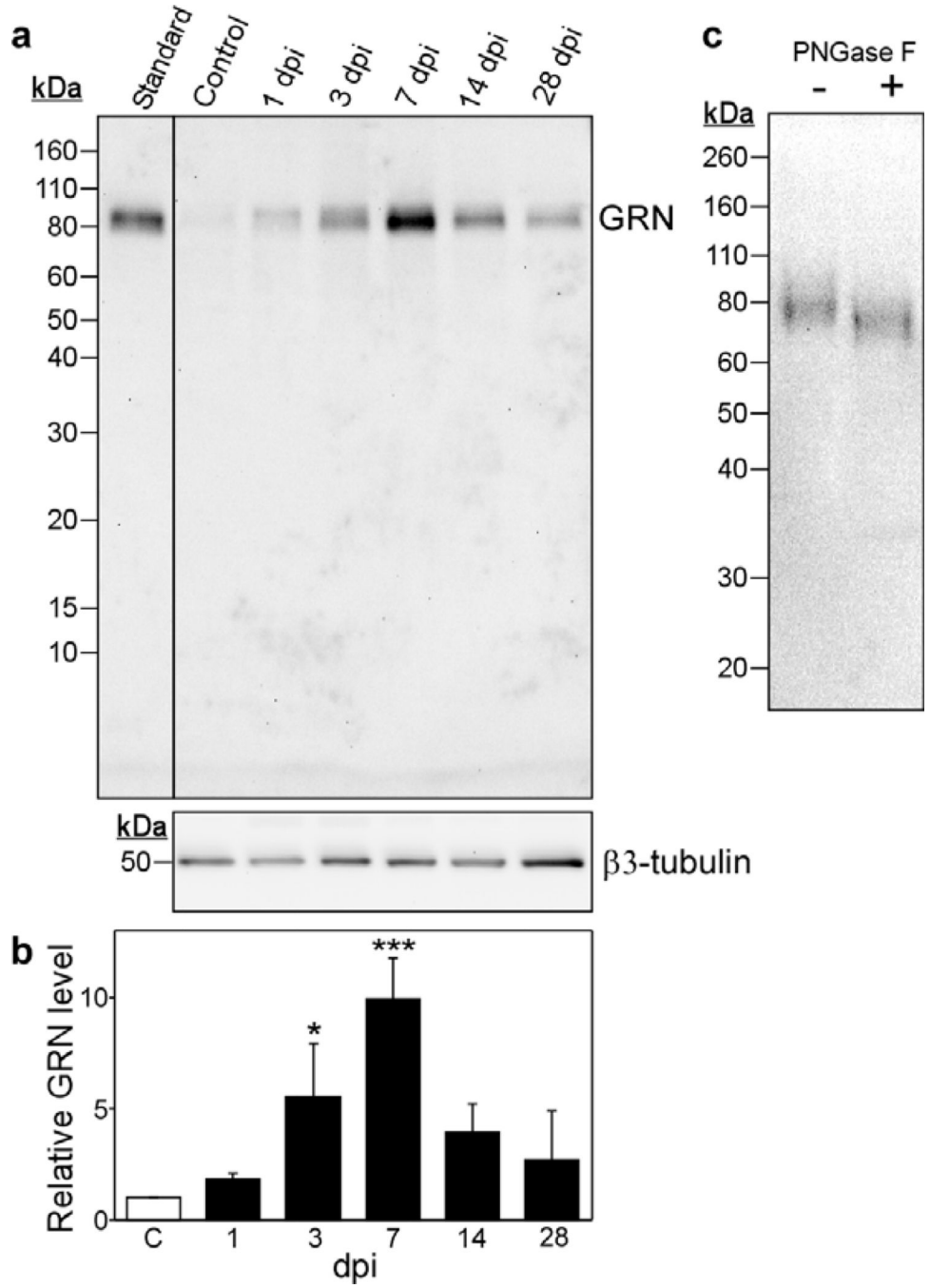

Fig. 3. Post-injury GRN expression increases at the protein level

(**a**) Levels of GRN protein in homogenates of injured and laminectomy control spinal cords were assessed by immunoblot analysis (10 – 20% gradient acrylamide gel) with anti-GRN and antibody. The resulting staining pattern was calibrated with prestained markers (shown in units of kDa on left) and conditioned medium from HEK293 cells expressing GRN (*standard*). β3-tubulin immunoreactivity served as loading control [34]. (**b**) GRN immunoreactivity was quantified by densitometry from triplicate immunoblots and normalized for β3-tubulin immunoreactivity. Results were then normalized to the

laminectomy control and plotted as relative GRN level ± SD as a function of dpi. GRN levels increased relative to the laminectomy control (C, *hollow bar*) by 3 dpi and reached a maximum near 7 dpi. GRN levels decreased thereafter but remained elevated above the laminectomy control. (*, $p < 0.05$; ***, $p < 0.001$ compared to the laminectomy control group; ANOVA with Dunnett's post hoc test). (**c**) Spinal cord homogenate prepared 7 dpi was incubated in the presence or absence of Peptide N-glycosidase F (PNGase F) followed by immunoblot analysis (10% acrylamide gel) with polyclonal anti-mouse GRN antibody. Tissue-derived GRN shifts to lower molecular mass in the presence of Peptide N-glycosidase F.

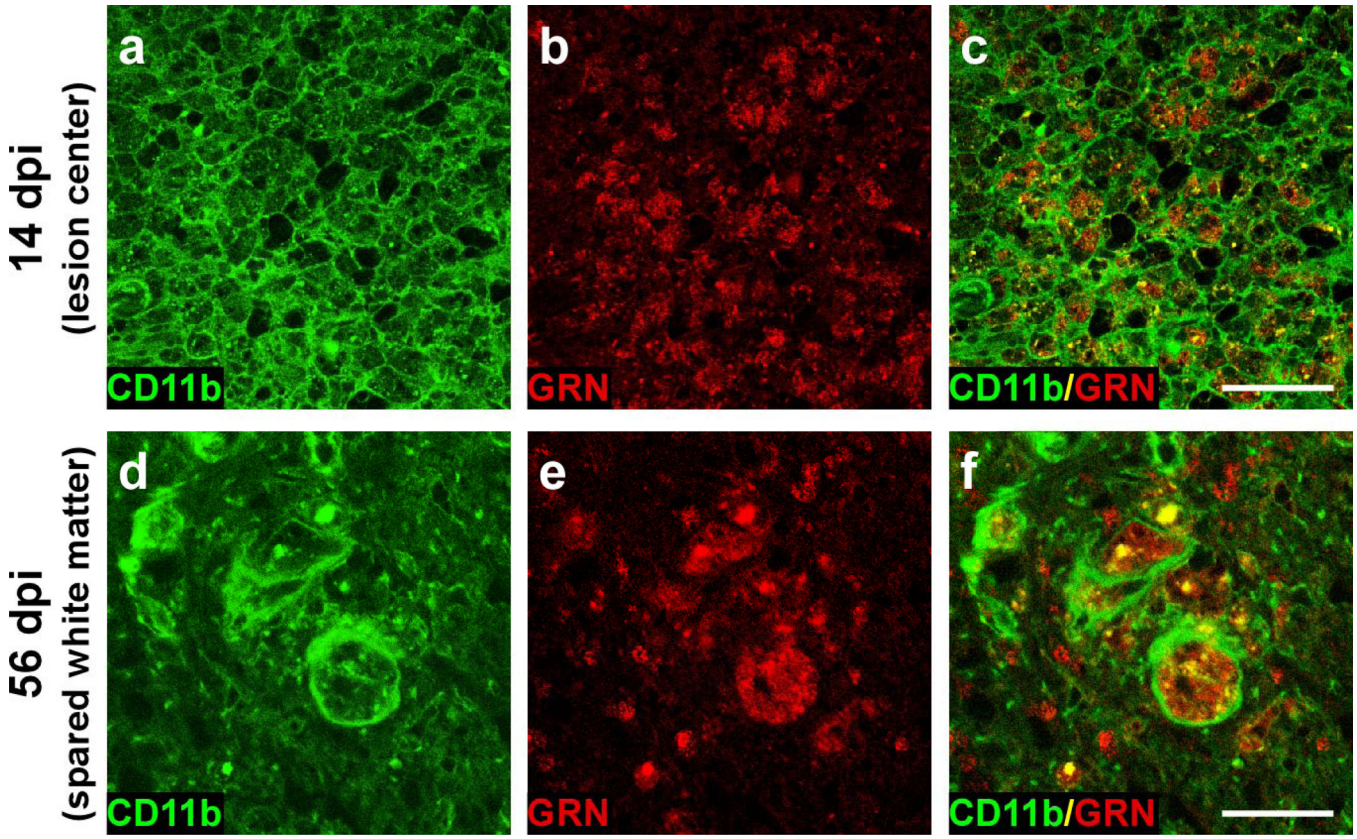

Fig. 4. Post-injury GRN expression occurs predominantly in macrophages and microglia

Double-label confocal images of transverse sections (at injury epicenter) labeled with CD11b to detect leukocytes (**a, d**) and anti-GRN antibody (**b, e**) at 14 dpi (gray matter) and 56 dpi (spared white matter). Merged images (**c, f**) reveal that nearly all GRN immunoreactive cells label positively for CD11b. Scale bar = 50 μm for panels **a–c** and 25 μm for panels **d–f**.

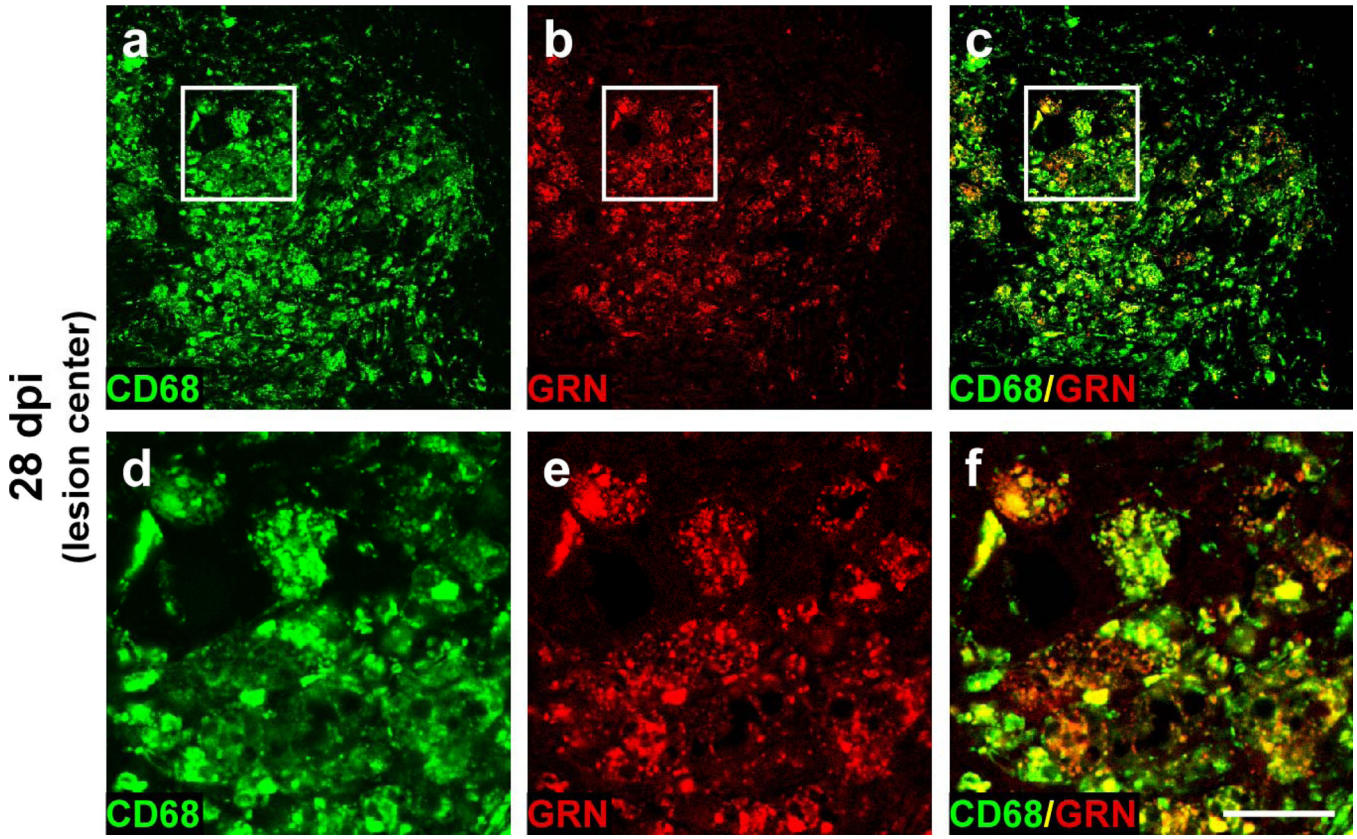

Fig. 5. Post-injury GRN expression colocalizes with lysosome-associated antigen CD68

Double-label confocal images of transverse sections (gray matter at injury epicenter) labeled with CD68 (**a, d**) to detect activated macrophages and microglia and anti-GRN antibody (**b, e**) at 28 dpi. Merged images (**c, f**) reveal that GRN associates with lysosomal-associated membrane protein CD68 in macrophage/microglia phagocytic vesicles. Panels **d, e** and **f** (scale bar = 25 μm) are magnified insets from images **a, b**, and **c** (scale bar = 100 μm), respectively.

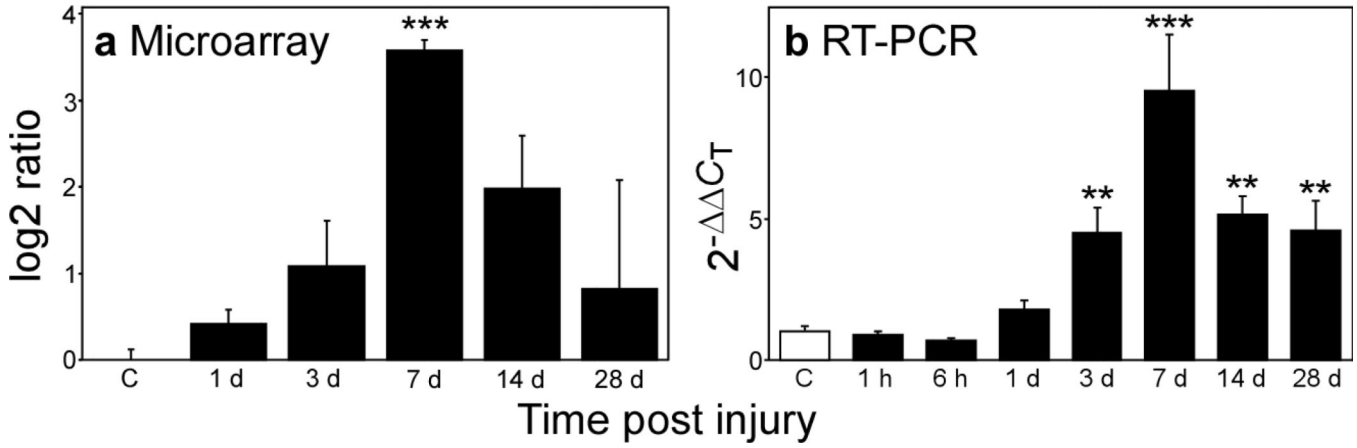

Fig. 6. Post-injury GRN expression increases at the mRNA level

Levels of GRN mRNA in homogenates of injured and laminectomy control (C, *hollow bar*) spinal cords were assessed by microarray (**a**) and quantitative RT-PCR (**b**) analyses, and plotted as log 2 ratio and $2^{-\Delta\Delta C_T}$, respectively. Both methods reveal significant time-dependent increases in GRN gene expression after injury (**, $p < 0.01$; ***, $p < 0.001$ compared to the laminectomy control group; ANOVA with Dunnett's post hoc test).